74-22

June 6, 1974

Backscattering cross sections for a dielectric shell computed by means of a T-matrix formalism[†]

by

Bo Peterson

[†] This project was supported by the Swedish Institute of Applied Mathematics

Institute of Theoretical Physics

Fack

S-402 20 Göteborg 5

Sweden

Abstract

A T-matrix formalism is used to calculate the backscattering cross section for a dielectric shell bounded by two spherical surfaces. The cross section is studied as a function of the displacement of the centre of the inner sphere from the centre of the outer sphere and as a function of the angle to the axis of rotational symmetry. The wave length considered is chosen equal to the radius of the outer sphere and the calculations are performed for the values 0.5 and 0.8 of the ratio between the radii of the inner and outer spheres. The necessary formulas from the T-matrix formulation as developed by P.C. Waterman and later extended by B. Peterson and S. Ström are reviewed.

I. Introduction

In Refs. [1] and [2] Waterman has given a T-matrix description of acoustic and electromagnetic scattering from a single homogeneous scatterer. The boundary conditions on the scatterer can be of a fairly general nature and the surface of the scatterer has to satisfy certain fairly weak geometrical condtions. Monochromatic waves are considered and the T-matrix refers to expansions in spherical wave solutions of Helmholtz's equation. This T-matrix formulation has subsequently been extended to the case of an arbitrary number of homogeneous scatterers [3], [4] and an arbitrary number of layered scatterers [5], [6]. The extension is valid under fairly weak conditions on the configuration of the scatterers.

The expansions of the incoming and scattered fields in spherical wave functions, the corresponding T-matrix and the associated Q-matrix for a surface of a single homogeneous scatterer [2] are presented in section II together with the extension to multilayered scatterers with constant properties for the region between the closed surfaces [6] as well as configurations of two such scatterers. In this section also a multiple scattering picture and some helpful relations are given. A numerical example of a dielectric shell bounded by two spherical surfaces and of the size two times the wavelength is given in section III. Some remarks on the advantages and generality of the T-matrix formulation are given in section IV. Only the lossless case will be treated in this paper.

II. Basic results from the T-matrix formulation

Throughout this paper the T-matrices considered will refer to spherical monochromatic waves with the factor $\exp(-i\omega t)$ supressed. The fundamental expansion functions $\vec{\psi}$ are the outgoing spherical vector wave solutions to

$$(\nabla^2 + k^2)\vec{\psi} = 0 \tag{2.1}$$

explicitly given by:

$$\vec{\psi}_n \equiv \vec{\psi}_{\tau\sigma mn}(k\vec{r}) \equiv \gamma_{mn}^{1/2}\left(k^{-1}\nabla\times\right)^{\tau}\left(k\vec{r}\, Y_{\sigma mn}(\hat{r})\, h_n^{(1)}(kr)\right) \tag{2.2}$$

where $\tau = 1,2$, $\sigma = e,o$ ("even" or "odd"), $n = 1,2,3,\ldots\infty$, $m = 0,1,2,3,\ldots n$, and

$$\gamma_{mn} = \frac{\varepsilon_m (2n+1)(n-m)!}{4\pi n(n+1)(n+m)!} \qquad \varepsilon_0 = 1,\ \varepsilon_m = 2 \text{ when } m \neq 0 \tag{2.3}$$

$h_n^{(1)}(kr)$ is a spherical Hankel-function and

$$Y_{\left\{\substack{e\\o}\right\}mn}(\hat{r}) = P_n^m(\cos\theta)\left\{\substack{\cos m\varphi\\ \sin m\varphi}\right\}$$

where P_n^m is an associated Legendre function [7]. With the abbreviated index notation the incoming respectively scattered field are represented as:

$$\vec{E}^{inc} = \sum_n a_n \operatorname{Re}\vec{\psi}_n \tag{2.4}$$

$$\vec{E}^{sc} = \sum_n f_n \vec{\psi}_n \tag{2.5}$$

where $\mathrm{Re}\vec{\psi}_n$ stands for the regular part of $\vec{\psi}_n$ i.e. the expression (2.2) with $h_n^{(1)}(kr)$ replaced by $j_n(kr)$, a spherical Bessel function. The solution of the problem is given by the T-matrix satisfying

$$f_n = \sum_{n'} T_{nn'} a_{n'} \tag{2.6}$$

In Ref. [2] it is shown that the T-matrix for a single homogeneous scatterer is of the form

$$T = -Q(Re,Re)Q(Out,Re)^{-1} \tag{2.7}$$

where Q(Re,Re) and Q(Out, Re) are matrices which are functions of the surface S of thescatterer and of the electric and magnetic properties of the scatterer. In the lossless case the T-matrix itself is well suited for numerical tests because it has to satisfy the following two relations

$$T^{\dagger}T = -\text{Realpart of } T \tag{2.8}$$

$$T^{t} = T \tag{2.9}$$

where † stands for hermite conjugation and t for transposition. The lossless case is described in Ref. [2] and carried through numerically in Refs. [8] and [9] by means of a procedure in which (2.8) and (2.9) are considered as subsidiary conditions, the explicit inversion of the Q-matrix being avoided by forming the unitary equivalent. The fundamental matrix Q(,) for a surface S as in Fig. 1 is given by:

$$Q(Re,Out) \equiv k_1 \int_S d\vec{s} \cdot \left[(\nabla \times Re\vec{\psi}_n(k_1\vec{r})) \times \vec{\psi}_{n'}(k_2\vec{r}) + \right.$$

$$\left. + \frac{\mu_1}{\mu_2} Re\vec{\psi}_n(k_2\vec{r}) \times (\nabla \times \vec{\psi}_{n'}(k_2\vec{r})) \right] \tag{2.10}$$

where k_1, μ_1 and k_2, μ_2 are the wave vector and magnetic permeability outside respectively inside the surface and $\vec{ds}$ is the outward pointing normal surface element.

Corresponding expressions Q(Out, Re), Q(Out, Out) and Q(Re, Re) are formed easily noting that the first argument act on the functions $\vec{\psi}_n(k_1\vec{r})$ and the second on functions $\vec{\psi}_n(k_2\vec{r})$. With this slightly more general definition of the Q-matrix than that given in Ref. [2] it is possible to cover most scattering configurations with constant material properties between surfaces, including of course the case of infinitely conducting surfaces. The infinitely conducting case is obtained by putting $\mu_2\varepsilon_2 = \mu_1\varepsilon_1$ $(k_1=k_2)$ and then taking $\lim_{\varepsilon_2\to 0} \frac{\mu_2}{\mu_1} Q$.

The T-matrix formalism is by no means restricted to homogeneous single scatterer. The most direct extension is to the multilayered scatterer, Fig. 2. The T-matrix T^{12} for the whole object is given by the Q-matrices Q^1 associated with the outer surface S_1 and the T-matrix T^2 for the rest of the object inside surface S_2, taking into account that T^2 is the T-matrix in a medium characterized by ε_2 and μ_2 [6].

$$T^{12} = -\left[Q^1(Re,Re)+Q^1(Re,Out)T^2\right]\left[Q^1(Out,Re)+Q^1(Out,Out)T^2\right]^{-1} \quad (2.11)$$

An iterative procedure for a multilayered scatterer starts by calculating the T-matrix for the innermost surface and the different Q-matrices for the next surface. Then the T-matrix for the two inner surfaces is constructed as in (2.11). The procedure is continued to the outermost surface. If the innermost surface is infinitely conducting the corresponding T-matrix is performed as was pointed out above. The T-matrix for the homogeneous case is, of course, reached by putting $T^2=0$ in (2.11). The formula (2.11) can be rewritten as

$$T^{12} = \left[T(1) - Q^1(Re, Out)\, T^2\, Q^1(Out, Re)^{-1}\right] \cdot$$

$$\left[1 + Q^1(Out, Out)\, T^2\, Q^1(Out, Re)^{-1}\right]^{-1} \qquad (2.12)$$

where

$$T(1) = -\, Q^1(Re, Re)\, Q^1(Out, Re)^{-1} \qquad (2.13)$$

is the T-matrix of a homogeneous scatterer bounded by the surface S_1 and media constants ε_1, μ_1 and ε_2, μ_2 outside respectively inside the surface. The terms obtained by a formal expansion of the inverse in (2.12) can be interpreted as various multiple scattering contributions to the total T-matrix [6]. In such an expansion there occur, besides the individual T(i) matrices, Q^1 matrices which, in accordance with the form of T(1), can be associated with a passage of a wave going out through S_1. Thus a $(Q^1)^{-1}$ factor is associated with a passage in through S_1 and a factor (with the appropriate arguments of the Q^1:s) $(Q^1)^{-1} \cdot Q^1$ with a reflection at the inside of S_1. The first few terms in the expansion of (2.12) can be depicted as in Fig. 3 and one easily sees that in general one has exactly the terms expected from a multiple scattering picture.

The extension of the results above to the case of several multilayered scatterers is given in detail in Ref. [6] (cf. also [4]). An essential point in this extension is the use of the translation properties of the different wave functions. The total transition matrix T^{12} for two different multilayered scatterers situated at $\vec{a}_1$ respectively $\vec{a}_2$ with the corresponding T-matrices T(1) respectively T(2) (see Fig. 4) is given by [6], [4]:

$$T^{12} = R(\vec{a}_1)T(1)\left[1 - \nabla(-\vec{a}_1+\vec{a}_2)T(2)\nabla(-\vec{a}_2+\vec{a}_1)T(1)\right]^{-1}\cdot$$

$$\cdot\left[1+\nabla(-\vec{a}_1+\vec{a}_2)T(2)R(\vec{a}_1-\vec{a}_2)\right]R(-\vec{a}_1)+$$

$$+R(\vec{a}_2)T(2)\left[1-\nabla(-\vec{a}_2+\vec{a}_1)T(1)\nabla(-\vec{a}_1+\vec{a}_2)T(2)\right]^{-1}\cdot$$

$$\cdot\left[1+\nabla(-\vec{a}_2+\vec{a}_1)T(1)R(\vec{a}_2-\vec{a}_1)\right]R(-\vec{a}_2) \qquad (2.14)$$

where R and σ are such that

$$\vec{\psi}_n(k(\vec{r}+\vec{c})) = \begin{cases} \sum_{n'} \nabla_{nn'}(\vec{c})\,\mathrm{Re}\,\vec{\psi}_{n'}(k\vec{r}) & r<c \\ \sum_{n'} R_{nn'}(\vec{c})\,\vec{\psi}_{n'}(k\vec{r}) & r>c \end{cases} \qquad (2.15)$$

The difference between R and σ is that σ has a Hankel function $h_1^{(1)}(kc)$ where R has a Bessel function $j_1(kc)$. Note that "Realpart of σ" = R [4]. Formula (2.14) is constructed under the assumption that $|\vec{a}_i - \vec{a}_j| > r_j''$ for $1,2 = i \neq j = 1,2$ where r_j'' is the radius from $\vec{a}_j$ to the surface S_j (cf. Fig. 4).

The terms obtained by a formal expansion of the inverses in (2.14) can be interpreted as various multiple scattering contributions of the total T-matrix, [4] see Fig. 5. In this way it is also seen that the two terms in (2.14) correspond to waves scattered in all possible ways between the scatterers and the last time scattered by scatterer number 1 respectively

scatterer number 2. It is also apparent that if $T(2) \to 0$, then $T^{12} \to R(\vec{a}_1)\, T(1)\, R(-\vec{a}_1)$ and correspondingly for the case $T(1) \to 0$.

III. A numerical application to a dielectric shell

As an application of the T-matrix formalism described in the previous section the backscattering cross section for a layered dielectric object with two spherical surfaces is calculated. (We are indebted to Dr. K. Östberg for the suggestion to consider this case; cf. Ref. [11] for a discussion of the corresponding concentric dielectric shell.) The radius of the outer and inner sphere are denoted by b and a respectively. The greater sphere has its centre at the origin and the smaller sphere has its centre at $c\hat{z}$. The material constants are: outside the greater sphere μ_1, ε_1, between spheres μ_2, ε_2, and inside smaller sphere μ_3, ε_3. The materials are such that $\mu_1=\mu_2=\mu_3$, $k_2=2k_1=2k_3$. In Figs. 6, 7, 8 and 9 the normalised cross section $= \lim_r \frac{4\pi r^2 |\vec{E}^s|^2}{\pi b^2 |\vec{E}^i|^2}$ is given for backscattering as a function of the angle between the incoming wave vector and the positive z-axis. The incoming wave is a plane wave with the electric vector orthogonal to the z-axis. The product $k_1 b$ is equal to 2π in the diagrams, the ratio c/b is chosen as a parameter, and the ratio a/b is 0.5 in Figs. 6.7 and 0.8 in Figs. 8.9. The calculations are made using formula (2.11) and the T-matrix for the inner sphere is transformed to the origin by means of the R-matrix in (2.15). As a check of the numerical approximations the relations (2.8) and (2.9) were tested and compared with the maximal element of T (see Fig. 10) for azimut index one. It might be noted that the program for this case with the whole T-matrix (15×28^2 elements) fill up all of a IBM 360 machine. The program was run in two steps. First the T-matrices were calculated for different ratios c/b, which were stored on a tape, then the differential cross sections were calculated reading the T-matrices from the tape. Of course the programs could have been made smaller by not taking all azimut indices together, but this could not have been used to calculate $\bar{\bar{T}}$ matrices with greater dimension. This is so because the translation matrices were calculated in such a way that all the needed 3-j symbols were calculated explicitly. This pro-

cedure contains big factorials which had to be lower than 56! because of the machine. A recurrence relation for the product of two 3-j symbols, which will lower the computational time, is used in Ref. [10]. Presumably this procedure also would permit an easier handling of the 3-j symbols in the present case.

The curves in Figs. 6 and 7 show more sturcture than those of Figs. 8 and 9 as might be expected since there is room for more wavelengths between the surfaces in the case a/b = 0.5. In Fig. 8 and 9 the minima become deeper and the maxima become higher for increasing c. From Fig. 10 it can be seen that the truncation error is largest for the inner T-matrix in the case a/b = 0.8. As explained above we were not able to increase the dimension of this T-matrix. However, as expected there will be a certain shielding from the dielectric shell which will diminish this error which doesn't seem to effect the total T-matrices as seen in Fig. 10. The tests for the T-matrices in the case of maximal translation (c = b - a) are as good as could be expected. It is to be noted that in the case of a/b = 0.5 the corresponding maximal "effective" translation distance (taking the value of the dielectric constant into account) is very big and the dimension needed increases with increasing translation.

IV. Concluding remarks

In scattering problems one usually first calculates the induced surface fields due to the incoming field, then out of the surface field, the scattered field is calculated. The advantage of the T-matrix formalism [1], [2] is that it allows one to jump over the step of calculating the surface fields. Instead the surface fields are expanded in spherical functions and then the unknown expansion coefficients are eliminated by means of the two equations for the integral representation of the field inside and outside the scatterer [1], [2].

One great advantage with the T-matrix formulation is that once the T-matrix is calculated, the scattered field, outside the smallest sphere including the scatterers and with centre at origin, can be calculated for every incoming wave (not necessarily a plane wave). In Refs. [5] and [6] and in the above it has been assumed that the source is situated outside the scatterers but this is not necessary. In fact, one could take the most general configuration of multilayered scatterers and put a surface outside the whole configuration including the source and immerse this in a medium including other multilayered scatterers and so on. The T-matrix itself also contains information about the numerical accuracy and consistency, because of the relations (2.8) and (2.9), which can be of great help especially for fully dielectric multilayered scatterers.

Programs for rotational symmetric infinitely conducting scatterers have been given by Waterman and McCarthy in Refs. [8] and [9]. Programs for lossless rotationally symmetric multilayered scatterers can be developed by moderate extensions of Waterman's programs. Translation matrices for $\vec{\psi}_n$ and $\mathrm{Re}\vec{\psi}_n$ can be found in Ref. [4] where also the formalism for an arbitrary number of scatterers is described in greater detail.

The T-matrix formulation based on the functions $\vec{\psi}_n$ and $\mathrm{Re}\vec{\psi}_n$ of course has the disadvantage of a slow rate of convergence for objects of size more than two to three times the wavelength. However, the general structure of

most of the formulas are valid for large classes of complete systems of expansion functions, i.e. in particular also for the case of functions possessing the opposite convergence property. (i.e. faster convergence for greater ratio objectsize/wavelength.) This aspect of the formalism deserves much further study.

Acknowledgement

I am grateful to Dr. Staffan Ström for careful reading of the manuscript.

References

1. P.C. Waterman, J. Acoust. Soc. Am. 45, 1417 (1969).

2. P.C. Waterman, Phys. Rev. D3, 825 (1971).

3. B. Peterson and S. Ström, J. Acoust. Soc. Am. (1974) (to appear).

4. B. Peterson and S. Ström, Phys. Rev. D8, 3661 (1973).

5. B. Peterson and S. Ström, Matrix formulation of acoustic scattering from multilayered scatterers, to appear.

6. B. Peterson and S. Ström, T-matrix formulation of electromagnetic scattering from multilayered scatterers, Phys. Rev. (to appear).

7. A.R. Edmons, Angular Momentum in Quantum Mechanics, Princeton University Press 1957.

8. P.C. Waterman and C.V. McCarthy, Numerical Solution of Electromagnetic Scattering Problems (Mitre, June 1968).

9. P.C. Waterman, Numerical Solution to Electromagnetic Scattering Problems in R. Mittra (Ed.): Computer Techniques for Electromagnetics (Pergamon, Oxford, 1973).

10. J.H. Bruning and Y.T. Lo, IEEE Trans. Ant. Prop. Vol. AP-19, No. 3, May 1971.

11. K. Östberg, Calculation of electromagnetic backscattering from a spherical dielectric shell. FOA 3 report C 3777-E1 February 1974.

Figure captions

Fig. 1 Notations for a homogenous scatterer.

Fig. 2 Notations for a multilayered scatterer.

Fig. 3 Multiple scattering interpretation of Eq. (3.2).

Fig. 4 Geometrical configuration for two scatterers.

Fig. 5 Multiple scattering interpretation of Eq. (3.4).

Fig. 6 Normalized differential backscattering cross section for a dielectric sphere, with $k_2 = 2k_1$ and radius b, enclosing a dielectric sphere of radius a=b/2, with $k_3=k_1$ and whose center is displaced the amount c along the positive z axis. All relative magnetic index (μ) are equal to one. The electric vector of the incoming field is orthogonal to the z-axis and the cross section is given for $k_1 b=2\pi$ as a function of the angle between the positive z-axis and the incoming wave vector for c/b=0:——, c/b=0.1:- - -, c/b=0.2:-·-·-, c/b=0.3 ···

Fig. 7 Same as in Fig. 6 but now with c/b=0.4:- - - -, c/b=0.5:-·-·-·.

Fig. 8 Same as in Fig. 6 but now with a/b=0.8 and c/b=0:——, c/b=0.05:- - -, c/b=0.10:-·-·-.

Fig. 9 Same as in Fig. 8 but now with $\frac{c}{b}$=0.15:- - - -, $\frac{c}{b}$=0.20:-·-·-·-.

Fig. 10 Result of numerical tests for T-matrices.

Fig. 11 Numerical test for T-matrices.

FIG. 1

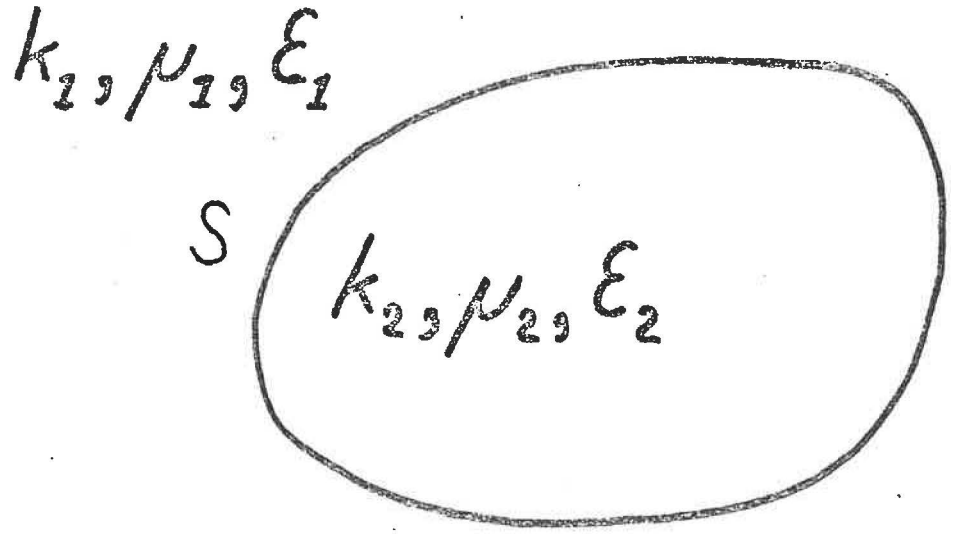
$k_1, \mu_1, \varepsilon_1$
S
$k_2, \mu_2, \varepsilon_2$

FIG. 2

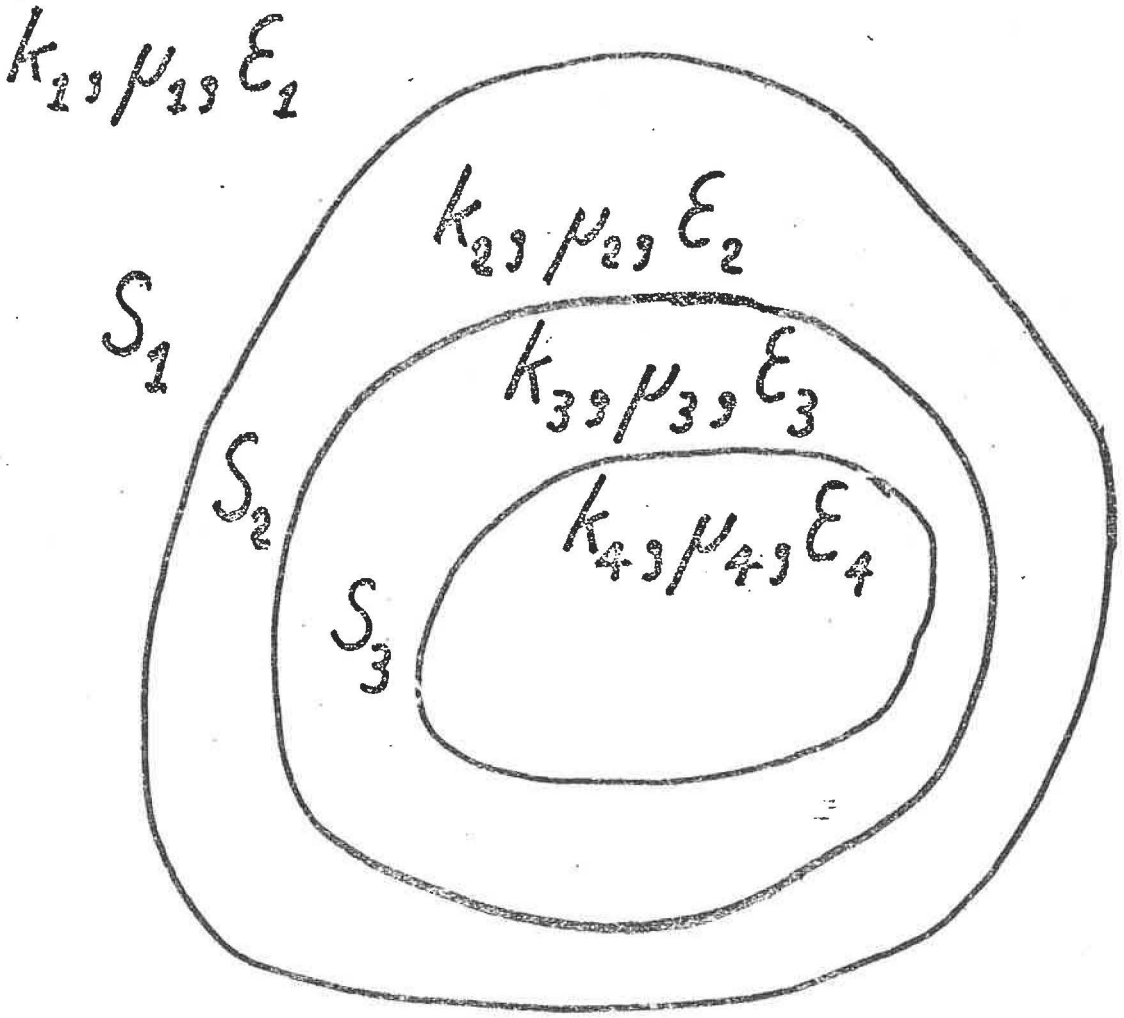
$k_1, \mu_1, \varepsilon_1$
$k_2, \mu_2, \varepsilon_2$
S_1
$k_3, \mu_3, \varepsilon_3$
S_2
$k_4, \mu_4, \varepsilon_4$
S_3

FIG. 3

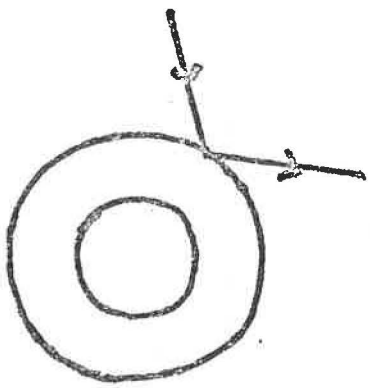

THE TERM $T(1)$

THE TERM $Q^1 T^2 [Q^1]^{-1}$

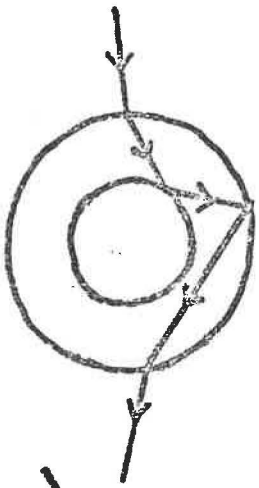

THE TERM $T(1) Q^1 T^2 [Q^1]^{-1} =$

$= - Q^1 [Q^1]^{-1} Q^1 T^2 [Q^1]^{-1}$

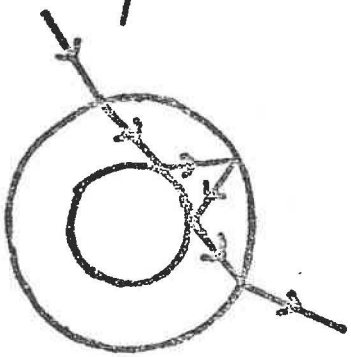

THE TERM $Q^1 T^2 [Q^1]^{-1} Q^1 T^2 [Q^1]^{-1}$

ETC.

FIG. 4

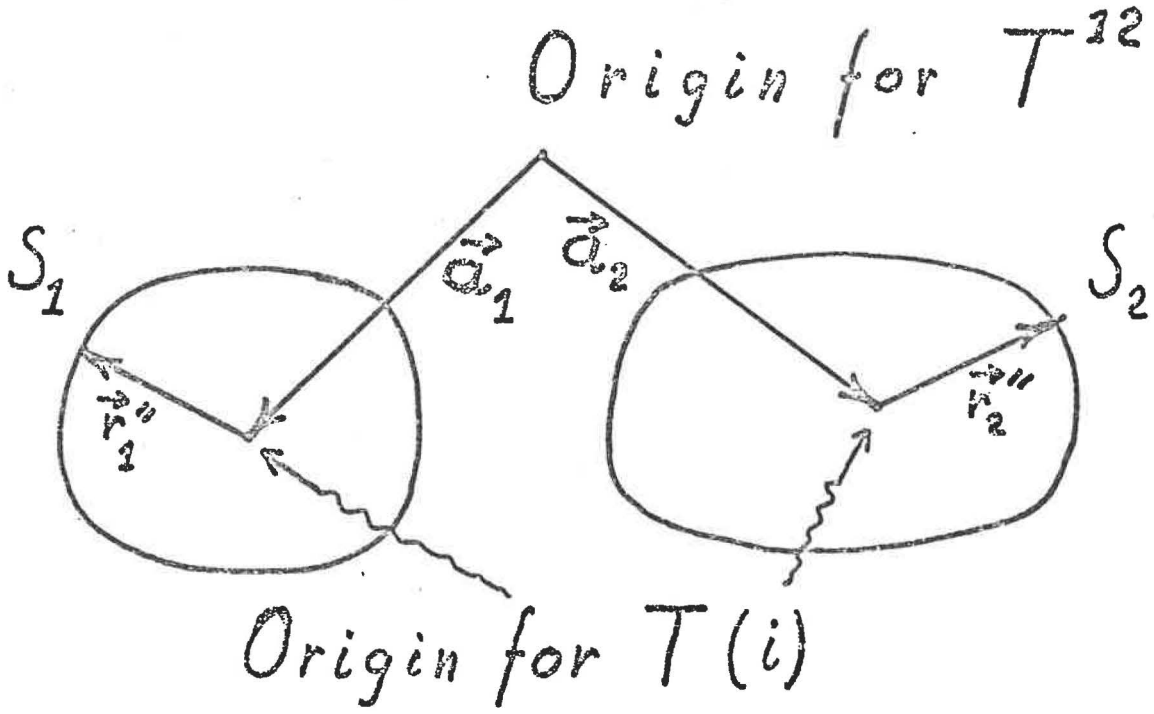

FIG. 5

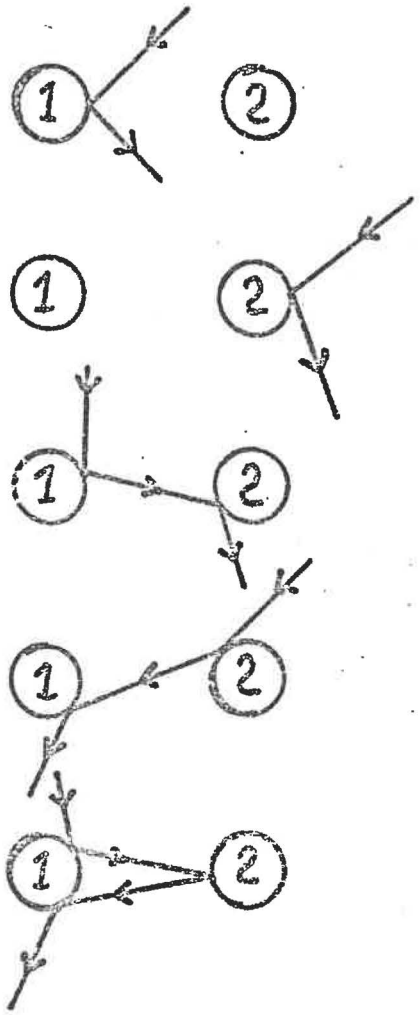

THE TERM $T(1)$

THE TERM $T(2)$

THE TERM $T(2)\nabla T(1)$

THE TERM $T(1)\nabla T(2)$

THE TERM $T(1)\nabla T(2)\nabla T(1)$

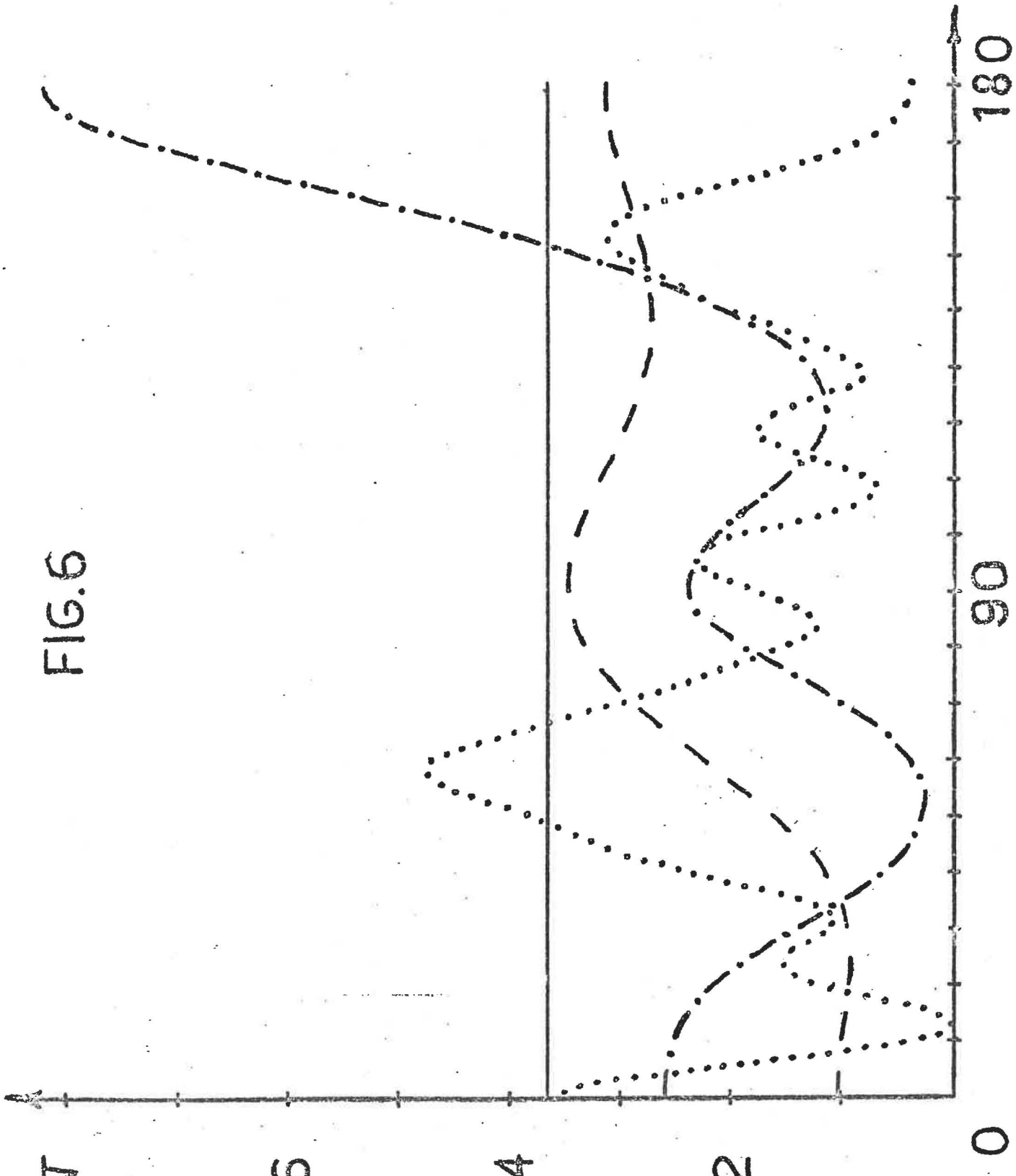

FIG.6

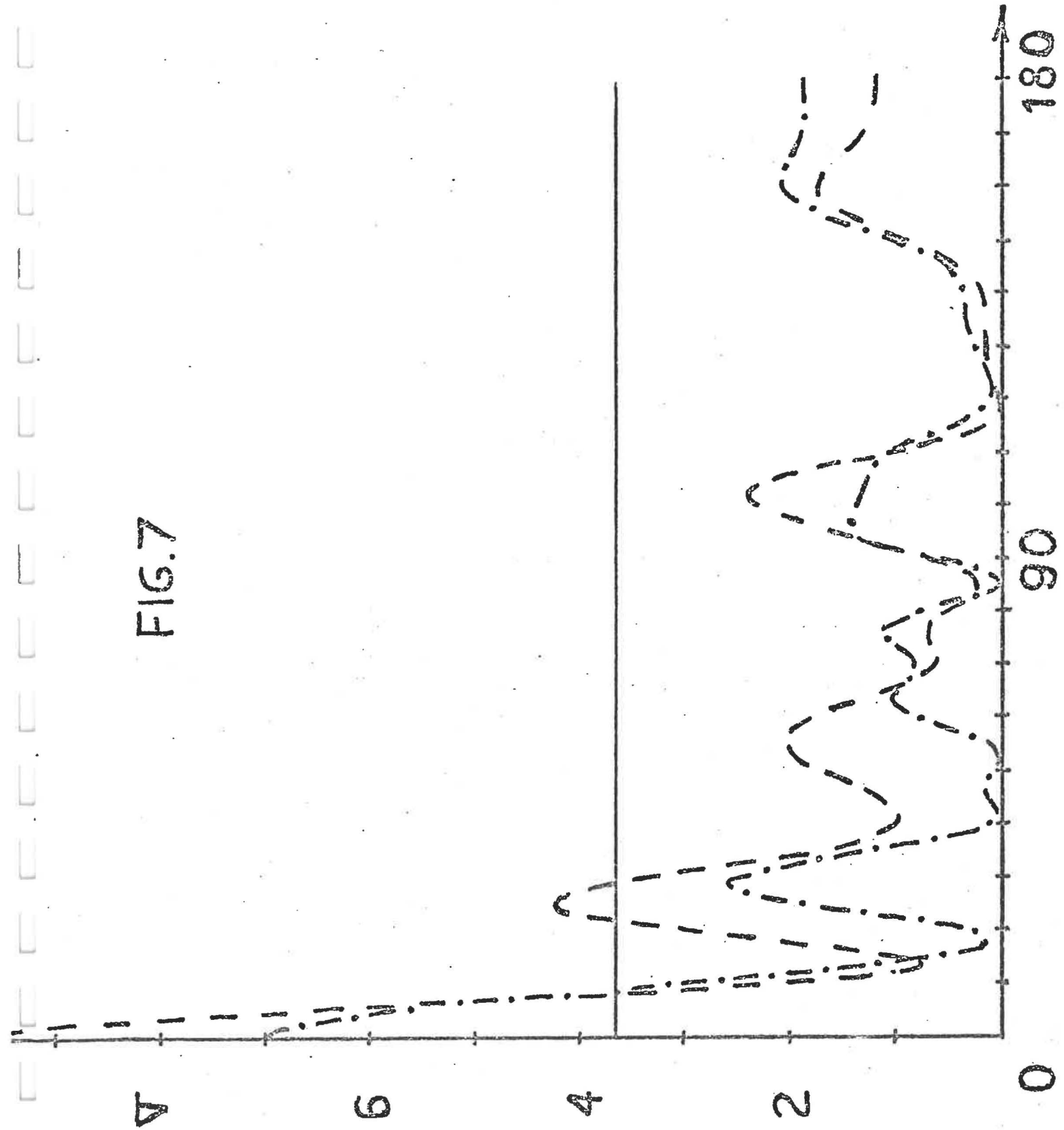

FIG.7

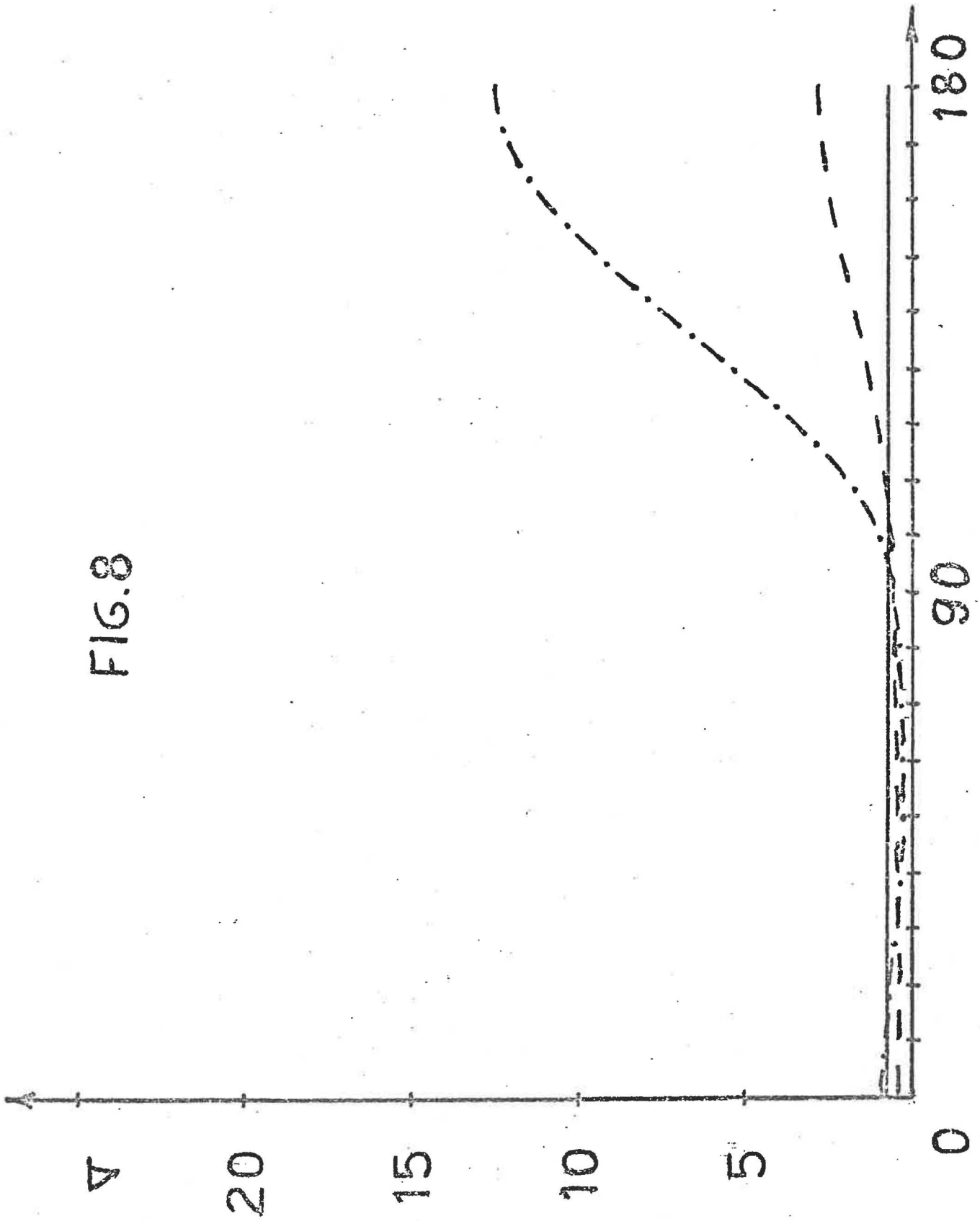

FIG.8

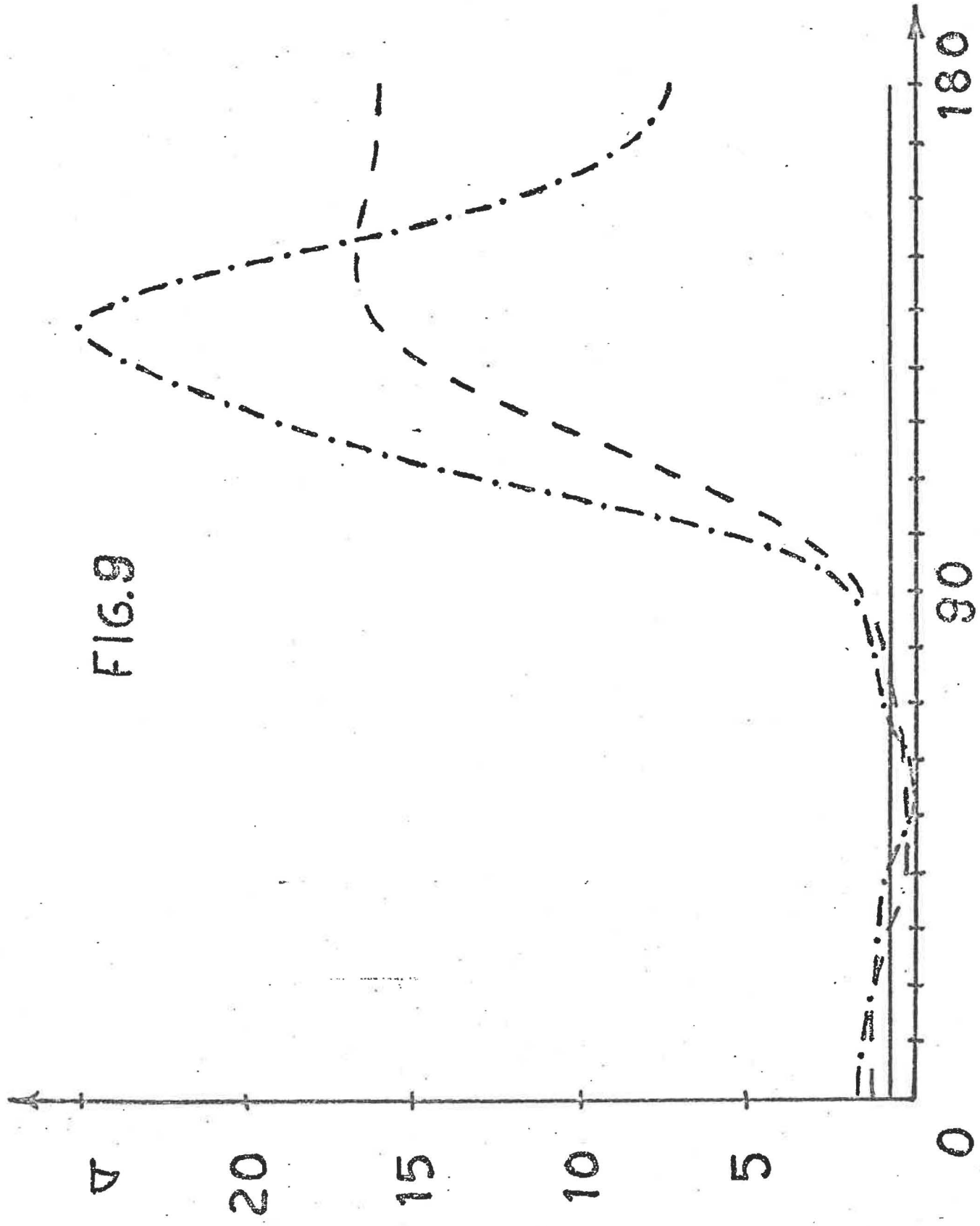

FIG.9

Fig. 10

Numerical tests.

Total and inner T matrix for $c = 0$.

$\frac{a}{b}$	$\max_{M=1} \lvert T_{IJ} \rvert$	$\min_{M=1} \lvert T_{IJ} \rvert$	T matrix
0.5	0.99	$2.0 \cdot 10^{-8}$	Total
0.5	1.0	$1.7 \cdot 10^{-8}$	Inner
0.8	1.0	$2.0 \cdot 10^{-8}$	Total
0.8	0.99	$1.4 \cdot 10^{-3}$	Inner

Total T matrix for $c = b - a$.

$\frac{a}{b}$	$\max_{M=1} \lvert T_{IJ} \rvert$	$\max_{M=1} \lvert Im(T^+T)_{IJ} \rvert$	$\max_{M=1} \lvert Re(T^+T+T)_{IJ} \rvert$	$\max_{M=1} \lvert (T^T-T)_{IJ} \rvert$
0.5	0.73	$6.2 \cdot 10^{-7}$	$1.2 \cdot 10^{-6}$	$< 10^{-14}$
0.8	0.91	$2.6 \cdot 10^{-7}$	$5.4 \cdot 10^{-7}$	$< 10^{-14}$